High performance thermoelectrics and challenges for practical devices

Qingyu Yan[1] and Mercouri G. Kanatzidis[2,*]

[1]*School of Materials Science and Engineering, Nanyang Technological University, Singapore, 639798, Singapore*

[2]*Northwestern University, Evanston 60208, Illinois, United States*

Thermoelectric materials can be potentially employed in solid-state devices that harvest waste heat and convert it to electrical power, thereby improving the efficiency of fuel utilisation. The spectacular increases in the efficiencies of these materials achieved over the past decade have raised expectations regarding the use of thermoelectric generators (TEG) in various energy saving and energy management applications, especially at mid-high temperature (400-900 ºC). However, several important issues that prevent successful TEG commercialisation remain unresolved in good part because of lack of a research roadmap.

The efficiency of a thermoelectric (TE) material is defined by the dimensionless figure of merit $ZT = S^2\sigma T/\kappa$, where S is the Seebeck coefficient, σ is the electrical conductivity, T is the operational temperature, and κ is the thermal conductivity composed of the electronic contribution (κ_{el}) and lattice contribution (κ_{lat}). However, the power conversion efficiency of a TE device (η) depends not on the ZT maximum at a given temperature, but on the average ZT (ZT_{ave}) over a wide temperature range as well as the temperature difference between the hot (T_h) and the cold source (T_c) as follows:

$$\eta = \frac{T_h - T_c}{T_h} \frac{\sqrt{1+ZT}-1}{\sqrt{1+ZT}+T_c/T_h}$$

Because these material properties (S, σ and κ) are interconnected through both the carrier concentration and electronic structure, the optimisation of any particular property is generally

performed at the expense of another property, which makes the achievement of high *ZT* values very challenging[1]. Effective routes to increasing *ZT* include electronic structure modifications such as electronic band structure engineering and the generation of extrinsic defects through alloying and nanostructuring to lower the lattice thermal conductivity.

A small but important commercial area where the first-generation TE devices and modules have already been successfully employed was the long-term space exploration conducted by the United States National Aeronautics and Space Administration (NASA) and the Soviet Union. Similar to the original Voyager 1 and Voyager 2 missions the recent Mars 2011 (rover Curiosity, November 2011) and 2020 missions (rover Perseverance, July 2020) are equipped with a radioisotope TE power system, and future Mars missions will also rely on the same system of electrical power generation. Using heat from the radioactive decay of plutonium oxide, this system produces dependable electricity that charges the rover's two primary batteries, and its TE modules are composed of the first-generation PbTe/tellurium–antimony–germanium–silver (TAGS) materials manufactured by Teledyne. The long-term reliability possible by TE generators (TEGs) was proven by these and other NASA missions where none has ever failed because of failure in the TE power generation system. After the long dormant period in research activity caused by the frustration over unsuccessful attempts to further enhance performance, TE materials have attracted significant attention from researchers during the past two decades. As a result, tremendous progress has been made in increasing the figure of merit. The field has bloomed with an outburst of new concepts and ideas that were subsequently implemented to break the four-decade old ZT records established in the 1950s and 1960s. The result was a new generation of materials developed since the early 2000s that significantly exceeded the expectations (the timeline of these advances is shown in **Box 1**). We note that there is considerable progress on development of organic, hybrid organic-inorganic, and inorganic thermoelectric materials and devices toward room temperature energy harvesting[2, 3, 4], which will not be discussed within the scope of this perspective because their ZT values are not on a comparable level yet to those of the inorganic counterparts. The new figures of merit achieved by the new materials

exceeded the old values by more than a factor of two and widely considered to be adequate for their implementation in modern TE devices with efficiencies greater than those of the state-of-the-art devices by more than 100%. However, the development of corresponding TE devices and modules that can transform heat to electricity using high-temperature sources operated between 400 and 900 °C has proceeded very slowly.[5] The question is 'why'?

Key developments in TE material improvement over the past 15 years

The "first-generation" materials employed in TE devices decades ago had power conversion efficiencies (PCE) of 3–6% in the temperature range of 300–1000 °C. The new materials could easily achieve PCE between 12 and 15%, which would be a remarkable breakthrough considering the conversion of low-quality energy (heat) to high-quality energy (electricity). It is reasonable to expect that such large PCEs would be commercially viable for a variety of applications. Practical TEGs can be divided into stationary and mobile ones. In the stationary generators, the hot side temperatures tend to be stable, and some parameters that may affect the device performance (such the overall weight and sensitivity to vibration) are typically relaxed. However, in mobile applications (such as those harvesting exhaust waste heat in vehicles), additional challenges include temperature fluctuations of the hot source and mechanical vibrations negatively affecting the device integrity and stability.

Various economic factors, such as the long-term uncertainty in the price of fossil fuels, are also stifling the development of TE devices on a commercial scale. For example, to recover waste heat in automobiles, the accrued energy savings can be used as electrical power to extend the vehicle mileage.[6] These savings must be substantial and significantly exceed the TEG cost. Over the past decade, crude oil price fluctuations resembled a rollercoaster, and their long-term average values exhibited a decreasing trend. Although it is difficult to accurately predict the price of crude oil, its value should sustainably well above current prices to stimulate utilisation of TE generators in automobiles. Because taxation strongly affects the fuel price, certain countries with high gasoline taxes may reach this level sooner than others.

Stationary applications of TEGs can involve large units installed in the industrial facilities[7] that are utilised for various manufacturing processes emitting large amounts of waste heat. To date, the number of commercially available TEGs is very small and affects only very few niche applications. These generators still use the first-generation materials, specifically bismuth telluride alloys and lead telluride.

The vehicles that can be considered viable candidates for the implementation of TEGs include semi-trucks, which run more a hundred thousand miles per year at a fuel economy of approximately six miles per gallon. Therefore, even at the 5% minimum energy savings achieved by TEG utilisation, approximately $6,000/y can be saved, which translates into $90,000 over the vehicle lifetime of ten to fifteen years. For personal vehicles, the savings would be considerably smaller.

What is holding back the development of high efficiency TEGs containing the new high-performance materials? The key technical obstacles are related to the thermal stability of the electrical contacts attached to the hot generator side; the mechanical stability and the long-term chemical stability of TE materials, which must be maintained for at least ten years; under the hot side.

It is interesting to compare the current development stage of TE technology, and little progress made in creating commercially viable energy converters, to the robust advances in the photovoltaics field. In the latter, the last two or three decades have also been transformational in the development of photovoltaic semiconductors with increased efficiency. This process has resulted in a flourishing and rapidly growing solar photovoltaic technology with falling costs and an industry with a market size of billions of dollars. What is particularly striking is the speed at which the recent emergence of perovskite halides as materials for solar cells has led to a budding industry currently on the cusp of commercialisation. The field of thermoelectrics has analogous advances in new materials

but there is a striking lag to the development of devices as mentioned above and very few researchers have the capability to fabricate TE power-generating devices.

Owing to the advances and breakthroughs in TE materials, this *perspective* discusses their potential to be implemented in devices and modules with a focus on TE power generation. After classifying the materials in terms of operating temperature, those most likely to be used in future devices are briefly discussed. We also discuss the key challenges and possible future strategies that can promote the further development of TE power generation technology, however, more extensive and comprehensive reviews can be found elsewhere.[5, 6, 8, 9 10] This perspective does not discuss TE cooling devices as they have existed for decades, and no corresponding enhancements in material performance have been achieved.

The powerful general design concepts devised more than a decade ago that have remarkably enhanced the performance of bulk TE materials are:[11] endotaxial nanostructuring involving the nucleation, growth, and spinodal decomposition processes that reduce the thermal conductivity of a material; electronic band alignment, electronic band convergence, resonance states, and electronic structure modification that enhance the power factor ($S^2\sigma$); and panoscopic all-scale architecturing that combines all beneficial effects into a single material system. In particular, proper band alignment is very important for achieving high power factors for two-phase nanostructured composites[12, 13]. In this case, a designed composition contains two separate phases with energy-aligned conduction or valence bands to facilitate carrier transport while actively scattering heat-carrying phonons. Electronic band convergence has been critical for tuning the electronic structure to achieve the maximum power factor. It involves the modification of separate electronic bands of the same carrier type aimed to converge their energies and substantially increase their contributions to carrier transport[13, 14]. Because each band makes its own contribution to the Seebeck coefficient on a weighted basis, strong enhancement can be achieved while maintaining high electrical conductivity. Some of the performance optimization process in 1st generation ternary TE

materials, e.g. $(Bi_{0.2}Sb_{0.8})_2Te_3$, is related to the band convergence, but was not referred to specifically as such.[15] The Pb-based chalcogenides (PbTe, PbSe, and PbS), filled skutterudites (REM_4Sb_{12}: RE = rare earth, M=Fe, Co, or Ni) and half–Heusler (HH) alloys are the key systems in which the above concepts led to superior performance characteristics. In terms of their ZT_{max} and ZT_{ave} values achieved during operation in the mid-temperature range, lead tellurides are the most promising materials, followed by complex filled skutterudites. However, in terms of mechanical strength (a key feature for the actual electronic devices), skutterudites and HH alloys are the most promising materials followed by tellurides. In addition to these concepts, there were discoveries of compounds with unprecedented ZT performance such as SnSe, MgAgSb, Mg_3Sb_2, $Yb_{14}MnSb_{11}$ and $La_{3-x}Te_4$.

This article is organised as follows. First, it discusses the recent advances in the development of high-performance TE materials, especially those with high stability, low manufacturing costs, and high scalability. Second, it describes the demand for novel TE device fabrication technologies based on these materials and the current state. Third, it considers the key challenges and possible strategies for transitioning to high efficiency devices and modules that will open the path to broader use and commercialization. Fourth, it concludes that the main reasons for the absence of available TE devices and modules based on the materials are knowledge gaps in how to develop stable high-temperature electrical and thermal interfaces.

The most important breakthroughs in new TE materials occurred in the mid-temperature range from 300 °C to approximately 650 °C, which matches the majority of heat sources suitable for energy harvesting and thus TE devices will produce the strongest impact. Above 650 °C, their implementation is considerably more challenging because the stability requirements become even more severe not only for the TE materials, but also for many other components of the devices and modules, including heat exchangers. Therefore, the prospects for harvesting the energy of high-temperature heat sources via solid-state TE technology are more remote than for mid-temperature sources. Leading materials systems for applications above 650 °C include the HH alloys $Nb_{1-x}Ti_xFeSb$ and $Nb_{1-x}Hf_xFeSb$ with a

ZT of ~ 1.5 at 1200 K[16, 17] and a promising ZT_{ave} of ~ 1 (500–1200 K)[16], $La_{3-x}Te_4$ with a ZT of ~ 1.2 at 1200 K [18] and $Yb_{14}MnSb_{11}$. with a ZT of 1.3 at 1223 K through suitable doping.[19]

TE modules from high performance materials and related challenges

General requirements for practical modules

To fabricate reliable TE power generation modules, it is important to realise very stable low-resistance electrical contacts (especially on the hot generator side) between the connecting electrodes and TE materials. A TE module is to be exposed to high temperatures, which can result in a chemical reaction and/or atomic diffusion at the electrode–material interface, leading to its instability and degradation. This extreme environment set in motion several complex phenomena that promote the development of detrimental secondary phases that reduce module conversion efficiency. Therefore, efficient and very stable diffusion barriers between the connecting electrodes and TE materials are required to prevent the chemical reactions and/or atomic diffusion. This is a nontrivial challenge because such barriers must also have low electrical contact resistance (in the magnitude of a few $\mu\Omega cm^2$) and be tailored to the specific TE materials. It requires a clearer fundamental understanding of these parasitic processes and more basic research on this subject. The coefficients of thermal expansion of TE materials, electrodes, barrier materials should match well to reduce thermomechanical stresses which degrade stability. One reason for the sparse basic research conducted in this area has been the broad perception that this essentially is an easily tractable device engineering problem that can be solved empirically. TE materials with good mechanical properties are critical for device modules with long service lifetimes. Vickers Hardness and Fracture Toughness are often used to gauge the mechanical performance of the TE materials. Some published works on TE devices, TE materials, module efficiency tests, have reported values of Vickers Hardness > 1 GPa and Fracture Toughness > 1 MPa $m^{1/2}$ which can serve as rough guide for the required mechanical properties for practical device applications, however, these may vary for different applications (e.g. stationary, mobile etc).

PbTe based modules

The so-called legacy (first-generation) PbTe-based modules developed in the 1960s and 1970s exhibited a PCE of 5.1% at T_h = 783 K and T_c = 366 K[20,21]. The efficiencies of the second-generation modules containing nanostructured PbTe-based materials (**Fig. 1a**) exceeded those by more than 100%. A low contact resistivity of below 10 mΩ cm was important for the minimisation of thermal losses. For example, modules constructed from p-type PbTe–MgTe (second generation, ZT ~ 1.9) and n-type PbTe (first generation) materials demonstrated PCE ~ 8.5% at T_h = 873 K and T_c = 283 K[22, 23]. Based on a simulated temperature distribution a subsequent segmented module was designed utilising legacy $Bi_{2-x}Sb_xTe_{3-y}Se_y$ alloys on the cold side of the TE legs to increase the PCE at lower temperatures up to 12% (**Fig. 1b**). The key to this successful demonstration was the fabrication process, which employed the pressure-assisted sintering of TE materials with diffusion barriers such as Fe and 80% Co-20% Fe-based alloys[23]. The theoretically predicted efficiency for this cascaded module was 15.6%, which included 23% losses experienced by an early experimental module due to the high resistance of electrode contacts. These losses pointed to the necessity of significant design improvements and were ultimately minimised to approximately 5–10% of the theoretical efficiency. Thermal cycling stability is another critical aspect of commercial applications. Generally, PbTe-based TE modules demonstrate good thermal stability at T < 793 K. In the PbTe–MgTe-based module, a slight decrease in PCE was observed during operation at T_{tot} = 873 K for 24 h, while no apparent changes were detected at $T_{hot} \leq$ 773.[23] The corresponding module comprising the nanostructured $Pb_{0.953}Na_{0.040}Ge_{0.007}Te$ p-type leg (**Fig. 1a**) with T_h and T_c maintained at 873 K and 283 K, respectively, produced 2 W with promising stability and ~12% PCE (**Fig. 1c-f**). In addition, the n-type $(PbSn_{0.05}Te)_{0.92}(PbS)_{0.08}$ TE material (ZT ~ 1.5) was used to build a uni-coupled module[24] by coupling with p-type $Ge_{0.87}Pb_{0.13}Te$ (ZT ~ 2.2). A high PCE of 12% was achieved at T_{hot} = 773 K, and T_{cold} = 323 K with P_{max} = 0.145 W, close to the theoretically predicted PCE of 13.6% and P_{max} = 0.16 W.

Te is a rare metal with an abundance of ~0.001 ppm in the earth crust, and is mainly obtained as the by-product of the electrolytic refining of Cu.[25] The annual production of Te is difficult to assess estimated to be ~1000 tons, which potentially can become a scale up bottleneck for TE devices using PbTe. Thus, the use of PbSe or PbS instead of PbTe in TE devices has been considered by researchers.[26, 27, 28, 29] The implementation of Pb(S, Se) materials would not only lower the costs, but because of their higher melting points they could increase the operational temperature for higher efficiency and results in higher Vickers hardness than PbTe. A recent report described a demonstration in a thermoelectric device with ZT_{max} in the range 1.5-1.9 at around 700-900K.[30] Using a heavily alloyed composition $Pb_{0.99-y}Sb_{0.012}Sn_ySe_{1-2x}Te_xS_x$ segmented with n-type Se-doped Bi_2Te_3 as the n-type leg and coupled with a typical p Na-doped PbTe segmented with $Bi_{2-x}Sb_xe_3$ as the p-type leg. An eight-couple module produced 3.1 W of power corresponding to the maximum conversion efficiency of 12.3% with ΔT = 507 K and current I = 3.7 A. The simulated highest conversion efficiency of the segmented module was 13.9% at a temperature difference ΔT = 513 K. The slightly lower efficiency compared to the theoretical one was attributed suboptimal electrical contact resistance. Here, too the use of Te may be problematic for broad based uses of Bi-Sb-Te compounds as the most used segmented modules for low temperature. Thus, alternative Te-free compounds are highly desirable. Recently, high efficiencies of 6.5~7.3% have been achieved at low temperatures (<593 K) for devices with Mg-Sb based compounds (e.g. Mg_3Sb_3[31] or $Mg_3(Sb, Bi)_2$[32]), which makes promising for scalable applications.

The high mechanical strength is rare in the top performing TE materials but is necessary for viable module fabrication. PbTe single crystals exhibit a low Vickers hardness of approximately 0.3 GPa, which can be increased to 0.8 GPa through Na doping[33]. Hot-pressed polycrystalline PbTe pellets containing 5–10mol% PbS possess a higher Vickers hardness values up to 1.2 GPa, which is still lower than those of skutterudite and HH alloys (3–4 GPa).[34] Further enhancements of the material mechanical strength are desirable to increase the resistance to mechanical fracture during operation. In this regard, replacing Te

with S or Se in PbTe as in $Pb_{0.93}Sb_{0.05}S_{0.5}Se_{0.5}$ which exhibits a Vickers hardness above 2.0 GPa is another advantage[23].

A study on PbTe evaporation revealed that for the device operated at T_{hot} = 793 K and T_{cold} = 333 K, some reduction in the cross-sectional area was observed due material sublimation occurred at distances of 0.5 and 1.1 mm from the hot generator side after 456 h[35]. This suggests that high thermal stability of TE devices can be achieved if a proper threshold is maintained for the high-temperature side. Recent studies on this topic are promising, such as those on Ga-doped PbTe-GeTe with $ZT_{average}$ = 1.27 between 400 and 773 K[36].

Skutterudite-based modules

Skutterudite-based TE materials have been favourites for TEGs because of attractive mechanical properties (corresponding to a Vickers hardness of 4 GPa and flexural strength up to 180 MPa for Yb-filled $CoSb_3$)[37] and sufficiently high *ZT* values.[38] A 4×4 leg device was built using $Yb_yCo_4Sb_{12}$ (*ZT* ~ 1.5) as the n-type component and $Ce_yFe_3CoSb_{12}$ as the p-type component achieved an energy conversion (η) of 8.4% with ΔT = 577 K and T_{hot} = 873 K[39]. An 8×8 leg device (**Fig. 2a**) using $CoSb_3$ as both the n-type (doped with Yb, Ca, Al, and Ga; *ZT* ~ 1.2) and p-type (doped with Pr, Ti, Ga, Ba, and Fe; *ZT* ~0.85) components has been fabricated as well[40]. The PCE and maximum power output (P_{max}) were ~9.1% and ~ 42 W at a current of ~15 A and ΔT of 600 K (**Fig. 2b**). In segmented TE modules composed of Bi_2Te_3/skutterudite[41], PCE reached ~12% with ΔT of 540 K.

The above-mentioned tests were performed in controlled gas environments (such as Ar or N_2). The results of a durability test conducted on skutterudite legs during thermal cycling in an open atmosphere revealed that their failure mainly resulted from oxidation and interlayer diffusion processes[42]. If crack generation occurs typically on the hot side of the TE legs, it increases the internal resistance and decreases the open circuit voltage (V_{oc}), **Fig. 2c**. Mitigation efforts include interfacial barrier layer and packaging protective against oxidation. A recent study on the screening of barrier layers involving density functional theory modelling revealed that Nb electrode could be used to effectively inhibit the interfacial reaction[43]. A

subsequent experimental study on such a skutterudite/Nb junction showed stable hot side interfacial resistance for up to 100 d at 848 K with PCE of 10.2% and P_{max} of 4.1 W at ΔT of 574 K, **Fig. 2d**. In addition to the above, Sb sublimation losses at T > 873 K causing composition changes represent a potential risk that degrades the performance of $CoSb_3$-based TE devices[44]. To minimise it the skutterudite-base materials can be chemically engineered to shift the *ZT* peak to lower temperatures. This concept was tested on two-leg devices[45] containing n-type $Yb_{0.25}Fe_{0.25}Co_{3.75}Sb_{12}$ (*ZT* ~ 1.3 at 740 K) and p-type $La_{0.7}Ti_{0.1}Ga_{0.1}Fe_{2.7}Co_{1.3}Sb_{12}$ (*ZT* ~ 0.97 at 760 K), which demonstrated an efficiency of 7.2% at a ΔT of only 366 K (T_{hot} = 679 K).

Half-Heusler modules

The half-Heusler HH compounds with the XYZ formula (X and Y: transition or rare earth metals, Z: p-block elements) exhibit robust mechanical strength, versatile composition, high thermal stability, and reasonably high *ZT* values. For these reasons, some of these materials can potentially be used in practical applications. However, their synthesis is a complex procedure due to the very high temperature and activation energy. The recent development of p-type HH materials with high *ZT* values considerably increased the efficiencies of the corresponding modules[46, 47]. A 4×4 leg TE device[47] with $FeNb_{0.88}Hf_{0.12}Sb$ (*ZT* ~ 1.5 at 1200 K) as the p-type leg and ZrNiSn *(ZT* ~ 1.0 at 950 K) as the n-type leg exhibits a PCE of 6.2% at ΔT = 655 K with T_{hot} = 1000 K, **Fig. 2e**. Here, Hf doping of the p-type legs is used to decrease the lattice thermal conductivity, however, Hf is expensive, and its use may lead to unfavourable material costs. To avoid Hf, Bi-doped ZrCoSn[48] and Ti-doped TaFeSb[49] have been proposed for p-type HH materials with *ZT* values of 1.4–1.5 at 973 K. The single-leg modules based on these HH alloys demonstrate PCEs of 9.0–11.4% in the T_{hot} of 823–973 K and T_{cold} = 300 K**, Fig. 2f**.

The optimisation of geometrical parameters is useful for minimising heat and electrical losses and predicting increases in η and P_{max}. This was done using finite element analysis for a 4×4 leg device consisting of n-type $Hf_{0.5}Zr_{0.5}NiSn_{0.98}Sb_{0.02}$ (*ZT* ~ 1.03) and p-type

$(Nb_{0.8}Ta_{0.2})_{0.8}Ti_{0.2}FeSb$ (ZT ~ 1.12).[50, 51] At close ZT values of the p-type and n-type legs in this example[47], a PCE of 8.3% and P_{max} of 8.5 W were reported for this single-stage TE device[51]. Segmented modules were prepared with n-type $Zr_{0.5}Hf_{0.5}NiSn_{0.985}Sb_{0.015}$ and p-type $Zr_{0.5}Hf_{0.5}CoSb_{0.8}Sn_{0.2}$ HH compounds on the hot side and Bi_2Te_3 on the cold side[50]. The obtained 4×4 leg device exhibited a record high PCE of 12.4% with a maximum area power density of 1.5 W/cm^2. Adding nanoparticles as inclusions to HH alloys to form nanocomposites is a promising method for reducing their thermal conductivity. A uni-coupled thermoelectric device fabricated from $(Hf_{0.6}Zr_{0.4})NiSn_{0.99}Sb_{0.01}$/W nanocomposite (n-type) and $Hf_{0.5}Zr_{0.5}CoSb_{0.8}Sn_{0.2}$ (p-type) possessed a PCE of 10.7% and area power density of 13.9 W/cm^2 with ΔT = 674 K[52]. This device exhibited no apparent performance degradation after 10 thermal cycles conducted between 373 and 1027 K. For successful commercialisation of HH alloy-based TE devices, the manufacturing costs must be low by avoiding expensive elemental components and developing a synthetic approach with a lower energy input. Although thermal cycling of HH alloy-based devices was performed in the past[52, 53], these cycles were either too few (only 10 thermal cycles were conducted for a $(Hf_{0.6}Zr_{0.4})NiSn_{0.99}Sb_{0.01}$/W-based TE device[52]) or performed at a too low temperature (up to 873 K for a $Zr_{0.5}Hf_{0.5}CoSb_{0.8}Sn_{0.2}$-based device[53]). Therefore, longer tests lasting thousands of hours at T_{hot} > 1000 K and post-mortem studies with a focus on the interfacial region close to the hot side are required to further understanding device reliability.

$Mg_2Sn_{1-x}Si_x$-based modules

$Mg_2Sn_{1-x}Si_x$-based TE devices have been widely explored due to several attractive features, including the presence of nontoxic elements. Encouraging results have been reported for the Mg_2Si TE devices with Ni electrodes prepared using a plasma-activated sintering technique, which exhibited no performance deterioration after aging for 1000 h.[54] Unfortunately, the effectiveness of the p-type counterpart of $Mg_2(Si,Sn)$ is very low (ZT ~ 0.7 at 750 K)[55]. The volatile nature of magnesium at moderately high temperatures results in phase instability, compositional changes, and degradation of the TE properties. Despite enormous efforts, these drawbacks have significantly limited commercial applications.[54, 56, 57, 58, 59, 60, 61] A single

leg (3.6 mm × 3.6 mm × 4.35 mm) of polycrystalline n-type Mg_3Sb_2-based material, in which $In_{52}Sn_{48}$ and $Ag_{56}Cu_{22}Zn_{17}Sn_5$ were used as brazes for the cold and hot sides, respectively, demonstrated a PCE of 10.6% at a temperature gradient of 400 K (T_{hot} = 773 K). This is among the highest efficiencies obtained for this temperature difference[62]. However, the large-scale application of Mg_3Sb_2-based generators is currently impeded by challenges related to the material and device fabrication procedures.

Nascent SnSe modules

The recent discovery of SnSe single crystals with record-breaking ZT values above 2.6 in the temperature range of 600–700 °C and their availability in both p-type and n-type forms have raised expectations for SnSe-based TE devices in the near future.[63, 64, 65, 66] This is particularly true in the light of new developments suggesting that polycrystalline compactions can achieve efficiencies close to those of single crystals. Currently, applications of SnSe in devices is limited by their poor mechanical properties of single crystals.[67] But the mechanical properties of polycrystalline SnSe are better (Vickers hardness: 669 MPa, flexural strength: 21 MPa, fracture toughness: 0.62 MPa $m^{1/2}$). To date, very few SnSe-based TEGs have been reported. A p-type polycrystalline SnSe-based power generator was built by a pseudo-three-dimensional (3D) printing method with a small peak output power of 20 μW with T_{hot} = 772 K (**Fig. 3a**)[68]. A recent study showed coupling n-type $Sn_{1-x}Pb_xSe$ legs (ZT=2.5) with p-type $Bi_2Te_{2.7}Se_{0.3}$ delivered a conversion efficiency of 4.4% with ΔT=200 K[69]. This efficiency is much lower than the expected value because of suboptimal electrical contact between the electrode and the legs. Therefore, finding effective metallisation layers is critical for SnSe-based devices. Initial results have highlighted how challenging it can be. For example, a single Ag metallisation layer was unable to inhibit the diffusion of Sn atoms into the Ag layer, resulting in a high contact resistivity of 7.03 mΩ·cm^2. Meanwhile, the application of a single Ni metallisation layer generated surface cracks because of the different thermal expansion coefficients of the various Ni-based compounds, such as $Ni_{17}Sn_3$, Ni_3Sn, and $Ni_{5.63}SnSe_2$[70]. An Ag/Co/Ti metallisation multilayer achieved a specific contact resistance of 1.53 mΩ·cm^2,

lower than that a single Ag layer, but still much higher than the contact resistances of commercial bismuth antimony telluride devices[71].

Cu_2Q (Q= S, Se, Te) modules

Cu_2Q p-type materials are highly promising TE materials with ZT = 1.5 at 1000 K for Cu_2Se and ZT = 1.7 at 1000 K for Cu_2S[72, 73]. These materials show good electronic transport properties and intrinsically low lattice thermal conductivities of the phonon–liquid electron–crystal frameworks. Unfortunately, the same liquid-like mobility also decreases stability due to electromigration of Cu ions in the samples destroying the TEG modules. This was deemed to be insurmountable and led to the termination of decade-long research studies mainly by NASA's Jet Propulsion Laboratory[74]. Recent strategies, however, employing electrically conductive but ion-blocking secondary phases or interfaces show that the long-range Cu ion electromigration can be hindered potentially allowing stable devices to be studied[75, 76, 77].

Potential $Yb_{14}MnSb_{11}$ modules

The $Yb_{14}MnSb_{11}$ compound is a promising material for power generation in the temperature range of 975–1275 K with a peak *ZT* of 1.0 at 1223 K[78]. The *ZT* value can be further increased to 1.3 at 1223 K through suitable doping.[19] $Yb_{14}MnSb_{11}$ shows good compatibility with other state-of-the-art p-type TE materials, which can be used to prepare segmented modules in various temperature ranges. A high PCE of 18.6% was predicted for a segmented p-type leg composed of $Yb_{14}MnSb_{11}$/$CeFe_4Sb_{12}$/TAGS/$(Bi, Sb)_2Te_3$ with ΔT = 975 K (T_{hot} = 1275 K and T_{cold} = 300 K)[78]. $Yb_{14}MnSb_{11}$ exhibits good mechanical properties (Vickers hardness: > 3 GPa)[79] and high thermal stability (no vapor losses up to 1395 K with La doping)[80], and can be produced by a scalable ball-milling process under Ar atmosphere[79]. However, no experimental testing of functional modules or single-leg devices fabricated from $Yb_{14}MnSb_{11}$ has been reported. The material would be almost exclusively used in space applications because of the cost-prohibitive nature of its composition.

Based on above discussion, a summary table I of the materials properties and device efficiency are shown below. For mid-high temperature operation, the thermal expansion matching is essential for module reliability. Because of the heavy atoms present the top-performing thermoelectrics, they tend to have a soft lattice nature and thus high thermal expansion coefficients. On the contrary the best metal electrodes have much lower ones by a factor of 2 to 4. How can such contacts achieve very low resistivity that must be maintained and survive the large temperature fluctuations? It is known that doping or adding secondary phases can tune the respective thermal expansion coefficients and this could be a way to mitigate these issues to a certain extend. It has been demonstrated, by matching the thermal expansion of n- and p- types Half-Heusler, the interfacial shear stresses can be reduced by 40% and significantly improve the reliability.[81] For segmented modules with Bi_2Te_3, both thermal expansion and dimension of the segment components should be consistent between n- and p-type legs. Therefore, continued innovations in design are needed to reconcile the thermally disparate materials.

Future research directions

Despite the tremendous progress in the field of TE materials for power generation, commercialisation and practical implementation of TEGs proceed very slowly. Currently, the fabrication of commercial Bi_2Te_3 π-type module is fully automated in each step and is capable for mass production. However, module fabrication using the newly developed high-ZT materials is not a trivial task and is required for practical TE power generation. There is a long way yet to go, before addressing the jugular issues, and a viable heat to electricity conversion industry for widespread TEG use. Beyond sporadic activities, no systematic basic research is being conducted to solve the problems blocking the full development of modules based on the new TE materials. Basic ongoing research focusing needs to be expanded beyond only increasing ZT to tackle all the other issues discussed above. Therefore, future research directions will need to be aimed at addressing simultaneously these key challenges all of which have to do with mechanical strength and interfaces. The mechanical and fracture strength of most high-performance thermoelectric materials is poor

with a few exceptions such as the HH alloys and perhaps the skutterudites (**Fig. 3b**). *Is it possible to raise the toughness and fracture strength of the new high ZT materials or to mitigate the risk of cracking during operation via innovative device design?* In general, most high-performing thermoelectric materials tend to have high thermal expansion coefficients whereas the best metal electrodes are low (**Fig. 3c**). The differences in thermal expansion coefficients across the interfaces of the materials in any given module will inevitably cause cracking at the interface and electrical discontinuities and will have to be reconciled. The development of metal electrodes matching the thermal expansion coefficients of TE materials will be required to create stable low resistance electrical contacts for high temperature operation. This can be realized either by alloying metals with various thermal expansion coefficient or by clever architectures design such as multiple layers. From Table I, the thermal expansion coefficient of TE materials (except Cu_2Se) usually ranges at 10-20 10^{-6} K^{-1}, while metals such as Cu, Ag, Ni, Co and Ti have a thermal expansion coefficient between 1 10^{-6} K^{-1} to 20 10^{-6} K^{-1},[82, 83] which makes the strategy possible. Electrodes with low resistance contacts must be achieved both at the high temperature and low temperature and of the thermoelectric leg. This is more difficult to achieve on the high temperature end of the device. The understanding of effective diffusion barrier layers to the electrode joints on the hot side is crucial. Obviously, there are other factors that go into overall mechanical strength such as yield strength and fracture toughness. These are properties for which we do not know much about for most of the high-performance thermoelectric materials as even small compositional modifications typically done to optimize ZT also change these. *What is the cutting-edge fundamental material science that needs to be done to try to increase the mechanical strength or at least learn to live with low strength by ingenious designing devices that are tolerant to this weakness?* The interface stability as a function of temperature, temperature fluctuations, and time will need to be understood at a fundamental level and controlled. Specifically, reactions between electrodes and TE materials and creation of new detrimental phases are the most worrisome. A moderate diffusion rate at the interface is essential for the formation of a strong interface, but a rather rapid or extensive one could lead to the unwanted degradation of TE materials. For development of stable metallization at

high temperature, high throughput methods should be a useful strategy to identify viable electrode systems.[43] The potential for chemical sublimation of TE materials during operation can be a problem and must be mitigated or suppressed by developing low-cost protective media including, various epilayers, as well as argon or helium gas (more conventional gases such as nitrogen or carbon dioxide can be also applied for this purpose). Solid insulation coatings containing silica, certain types of ceramics, phosphate glasses, and lead oxide enamels may decrease the sublimation rates of TE materials as well; however, the latter would require proper engineering to prevent failure due to rupture. In view of the above-mentioned key challenges for TE devising, a transverse TE device[84] is worth highlighting. In such devices, the electrical contacts are made only on the cold sides, which avoid the concerns on the instability of the interface and contact of the hot sides as in conventional devices. A high device ZT of ~0.7 has been achieved for Re_4Si_7 single crystal in a transverse TE device.[84] Such devices may not be applicable to all TE materials because it has special requirements for anisotropic transport properties along different crystal axis for p- and n-type carriers requiring single crystals. The subfield of transverse thermoelectrics is undeveloped as a result. For TE materials with symmetric crystal structures or polycrystalline nature, constructing multi-layer heterostructures may be necessary, where, however, only very low ZT values (~10^{-2}) have been demonstrated. Although there are additional issues to overcome including optimal thermal interfaces to efficiently guide the heat from the source through the devices and resist detachment, the aforementioned challenges are make-or-break propositions. These are not necessarily just engineering issues. There has to be considerable basic research focus to raise our fundamental understanding as tackling these challenges will define the lifetime of the TE modules which will have to be in the order of a decade or two. A scientific and technological research roadmap is needed to highlight necessary steps to transition from real advances in ZT research into a viable TEG technology. The stability, reliability and efficiency of thermoelectric devices and modules need to be measured reliably and this is not trivial. The development of TE modules and TEGs is in a similar state as the materials research was 20-30 years ago only the challenges are more severe. Therefore, such work currently is only being done in very few Laboratories

with home-build systems. The availability of easy to use commercial device and module measurement systems for use by non-specialists will produce reliable data that can be compared across different labs is is necessary. It may also be useful to establish third-party agencies for standard evaluation of the TE device performance, similar to what currently is done in photovoltaic device research, for reliable comparison between different materials and devices reported by different groups. In addition, several new engineering approaches have been developed to fabricate planar and vertical TE devices including laser direct sintering[85], tape casting[86], and vacuum filtration[87], where these methods still use Bi-Te commercial powder in device fabrication. Similar processing techniques could be adapted for the new TE materials. We are optimistic that future research focusing on bridging the chasm between the materials discovery and development on the one hand and the device/module engineering communities on the other will achieve meaningful advances in broad based module development.

References

1. Wood C. Materials for thermoelectric energy conversion. *Rep. Prog. Phys.* **51**, 459 (1988).
2. Nandihalli N, Liu CJ, Mori T. Polymer based thermoelectric nanocomposite materials and devices: Fabrication and characteristics. *Nano Energy* **78**, 105186 (2020).
3. Petsagkourakis I, Tybrandt K, Crispin X, Ohkubo I, Satoh N, Mori T. Thermoelectric materials and applications for energy harvesting power generation. *Sci. Technol. Adv. Mater.* **19**, 836-862 (2018).
4. Tarancon A. Powering the IoT revolution with heat. *Nat. Electron.* **2**, 270-271 (2019).
5. Jaziri N, Boughamoura A, Muller J, Mezghani B, Tounsi F, Ismail M. A comprehensive review of Thermoelectric Generators: Technologies and common applications. *Energy Reports* **6**, 264-287 (2020).
6. Kober M. Holistic Development of Thermoelectric Generators for Automotive Applications. *J. Electron. Mater.* **49**, 2910-2919 (2020).
7. Lan S, Yang ZJ, Stobart R, Chen R. Prediction of the fuel economy potential for a skutterudite thermoelectric generator in light-duty vehicle applications. *Appl. Energy* **231**, 68-79 (2018).
8. Zoui MA, Bentouba S, Stocholm JG, Bourouis M. A Review on Thermoelectric Generators: Progress and Applications. *Energies* **13**, 3606 (2020).
9. He R, Schierning G, Nielsch K. Thermoelectric Devices: A Review of Devices, Architectures, and Contact Optimization. *Adv. Mater. Technol.* **3**, 1700256 (2018).
10. Tan GJ, Ohta M, Kanatzidis MG. Thermoelectric power generation: from new materials to devices. *Philos. Trans. R. Soc., A* **377**, 20180450 (2019).
11. Sootsman JR, Chung DY, Kanatzidis MG. New and Old Concepts in Thermoelectric Materials. *Angew. Chem., Int. Ed.* **48**, 8616-8639 (2009).
12. Tan GJ, Zhao LD, Kanatzidis MG. Rationally Designing High-Performance Bulk Thermoelectric Materials. *Chem.*

Rev. **116**, 12123-12149 (2016).
13. Pei YZ, Shi XY, LaLonde A, Wang H, Chen LD, Snyder GJ. Convergence of electronic bands for high performance bulk thermoelectrics. *Nature* **473**, 66-69 (2011).
14. Zhao LD, Dravid VP, Kanatzidis MG. The panoscopic approach to high performance thermoelectrics. *Energy Environ. Sci.* **7**, 251-268 (2014).
15. Stordeur M, Stolzer M, Sobotta H, Riede V. Investigation of the Valence Band Structure of Thermoelectric $(Bi_{1-x}Sb_x)_2Te_3$ Single Crystals. *Phys. Status Solidi B* **150**, 165-176 (1988).
16. Fu C*, et al.* Realizing high figure of merit in heavy-band p-type half-Heusler thermoelectric materials. *Nat. Commun.* **6**, 8144 (2015).
17. Zou M, Li J-F, Kita T. Thermoelectric properties of fine-grained FeVSb half-Heusler alloys tuned to p-type by substituting vanadium with titanium. *J. Solid State Chem.* **198**, 125-130 (2013).
18. May AF, Fleurial JP, Snyder GJ. Thermoelectric performance of lanthanum telluride produced via mechanical alloying. *Phys. Rev. B* **78**, 125205 (2008).
19. Toberer ES*, et al.* Traversing the Metal-Insulator Transition in a Zintl Phase: Rational Enhancement of Thermoelectric Efficiency in $Yb_{14}Mn_{1-x}Al_xSb_{11}$. *Adv. Funct. Mater.* **18**, 2795-2800 (2008).
20. LaLonde AD, Pei Y, Wang H, Jeffrey Snyder G. Lead telluride alloy thermoelectrics. *Mater. Today* **14**, 526-532 (2011).
21. Rowe DM. *Thermoelectrics handbook: macro to nano*. (CRC press, Boca Raton, 2005).
22. Hu XK*, et al.* Power generation from nanostructured PbTe-based thermoelectrics: comprehensive development from materials to modules. *Energy Environ. Sci.* **9**, 517-529 (2016).
23. Jood P, Ohta M, Yamamoto A, Kanatzidis MG. Excessively Doped PbTe with Ge-Induced Nanostructures Enables High-Efficiency Thermoelectric Modules. *Joule* **2**, 1339-1355 (2018).
24. Hazan E, Ben-Yehuda O, Madar N, Gelbstein Y. Functional Graded Germanium–Lead Chalcogenide-Based Thermoelectric Module for Renewable Energy Applications. *Adv. Energy Mater.* **5**, 1500272 (2015).
25. Green MA. Rare materials for photovoltaics: Recent tellurium price fluctuations and availability from copper refining. *Sol. Energy Mater. Sol. Cells* **119**, 256-260 (2013).
26. Luo ZZ*, et al.* Soft phonon modes from off-center Ge atoms lead to ultralow thermal conductivity and superior thermoelectric performance in n-type PbSe-GeSe. *Energy Environ. Sci.* **11**, 3220-3230 (2018).
27. Luo ZZ*, et al.* Strong Valence Band Convergence to Enhance Thermoelectric Performance in PbSe with Two Chemically Independent Controls. *Angew. Chem., Int. Ed.* **60**, 268-273 (2021).
28. Lee Y*, et al.* Contrasting role of antimony and bismuth dopants on the thermoelectric performance of lead selenide. *Nat. Commun.* **5**, 1-11 (2014).
29. Hodges JM*, et al.* Chemical Insights into PbSe-x%HgSe: High Power Factor and Improved Thermoelectric Performance by Alloying with Discordant Atoms. *J. Am. Chem. Soc.* **140**, 18115-18123 (2018).
30. Jiang B*, et al.* High-entropy-stabilized chalcogenides with high thermoelectric performance. *Science* **371**, 830 (2021).
31. Zihang Liu*, et al.* Demonstration of ultrahigh thermoelectric efficiency of ~7.3% in Mg_3Sb_2/MgAgSb module for low-temperature energy harvesting. *Joule* **5**, 1196-1208 (2021).
32. Ying PJ*, et al.* Towards tellurium-free thermoelectric modules for power generation from low-grade heat. *Nat. Commun.* **12**, 1-6 (2021).
33. Gelbstein Y, Gotesman G, Lishzinker Y, Dashevsky Z, Dariel MP. Mechanical properties of PbTe-based thermoelectric semiconductors. *Scr. Mater.* **58**, 251-254 (2008).
34. Ni JE*, et al.* Room temperature Young's modulus, shear modulus, Poisson's ratio and hardness of PbTe-PbS

thermoelectric materials. *J. Mater. Sci. Eng. B* **170**, 58-66 (2010).
35. Sadia Y, Ben-Ayoun D, Gelbstein Y. Evaporation-condensation effects on the thermoelectric performance of PbTe-based couples. *Phys. Chem. Chem. Phys.* **19**, 19326-19333 (2017).
36. Luo ZZ*, et al.* High Figure of Merit in Gallium-Doped Nanostructured n-Type PbTe-xGeTe with Midgap States. *J. Am. Chem. Soc.* **141**, 16169-16177 (2019).
37. Zhou ZX*, et al.* Uniform dispersion of SiC in Yb-filled skutterudite nanocomposites with high thermoelectric and mechanical performance. *Scr. Mater.* **162**, 166-171 (2019).
38. Li WJ*, et al.* Enhanced Thermoelectric Performance of Yb-Single-Filled Skutterudite by Ultralow Thermal Conductivity. *Chem. Mater.* **31**, 862-872 (2019).
39. Zong PA*, et al.* Skutterudite with graphene-modified grain-boundary complexion enhances zT enabling high-efficiency thermoelectric device. *Energy Environ. Sci.* **10**, 183-191 (2017).
40. Nie G*, et al.* High performance thermoelectric module through isotype bulk heterojunction engineering of skutterudite materials. *Nano Energy* **66**, 104193 (2019).
41. Zhang QH*, et al.* Realizing a thermoelectric conversion efficiency of 12% in bismuth telluride/skutterudite segmented modules through full-parameter optimization and energy-loss minimized integration. *Energy Environ. Sci.* **10**, 956-963 (2017).
42. Skomedal G, Kristiansen NR, Sottong R, Middleton H. Evaluation of Thermoelectric Performance and Durability of Functionalized Skutterudite Legs. *J. Electron. Mater.* **46**, 2438-2450 (2017).
43. Chu J*, et al.* Electrode interface optimization advances conversion efficiency and stability of thermoelectric devices. *Nat. Commun.* **11**, 1-8 (2020).
44. Daniel MV, Friedemann M, Franke J, Albrecht M. Thermal stability of thermoelectric $CoSb_3$ skutterudite thin films. *Thin Solid Films* **589**, 203-208 (2015).
45. Li WJ*, et al.* High-Efficiency Skutterudite Modules at a Low Temperature Gradient. *Energies* **12**, 4292 (2019).
46. Fu CG, Zhu TJ, Liu YT, Xie HH, Zhao XB. Band engineering of high performance p-type FeNbSb based half-Heusler thermoelectric materials for figure of merit zT > 1. *Energy Environ. Sci.* **8**, 216-220 (2015).
47. Fu CG*, et al.* Realizing high figure of merit in heavy-band p-type half-Heusler thermoelectric materials. *Nat. Commun.* **6**, 1-7 (2015).
48. Zhu HT*, et al.* Discovery of ZrCoBi based half Heuslers with high thermoelectric conversion efficiency. *Nat. Commun.* **9**, 1-9 (2018).
49. Zhu HT*, et al.* Discovery of TaFeSb-based half-Heuslers with high thermoelectric performance. *Nat. Commun.* **10**, 1-8 (2019).
50. Xing YF*, et al.* High-efficiency half-Heusler thermoelectric modules enabled by self-propagating synthesis and topologic structure optimization. *Energy Environ. Sci.* **12**, 3390-3399 (2019).
51. Yu JJ*, et al.* Half-Heusler Thermoelectric Module with High Conversion Efficiency and High Power Density. *Adv. Energy Mater.* **10**, 2000888 (2020).
52. Kang HB*, et al.* Decoupled phononic-electronic transport in multi-phase n-type half-Heusler nanocomposites enabling efficient high temperature power generation. *Mater. Today* **36**, 63-72 (2020).
53. Bartholome K*, et al.* Thermoelectric Modules Based on Half-Heusler Materials Produced in Large Quantities. *J. Electron. Mater.* **43**, 1775-1781 (2014).
54. Sakamoto T*, et al.* Thermoelectric Behavior of Sb- and Al-Doped n-Type Mg_2Si Device Under Large Temperature Differences. *J. Electron. Mater.* **40**, 629-634 (2011).
55. Gao P, Davis JD, Poltavets VV, Hogan TP. The p-type $Mg_2Li_xSi_{0.4}Sn_{0.6}$ thermoelectric materials synthesized by a B_2O_3 encapsulation method using Li_2CO_3 as the doping agent. *J. Mater. Chem. C* **4**, 929-934 (2016).

56. Bux SK, Yeung MT, Toberer ES, Snyder GJ, Kaner RB, Fleurial J-P. Mechanochemical synthesis and thermoelectric properties of high quality magnesium silicide. *J. Mater. Chem.* **21**, 12259-12266 (2011).
57. Kato D, Iwasaki K, Yoshino M, Yamada T, Nagasaki T. Control of Mg content and carrier concentration via post annealing under different Mg partial pressures for Sb-doped Mg_2Si thermoelectric material. *J. Solid State Chem.* **258**, 93-98 (2018).
58. Inoue H, Yoneda S, Kato M, Ohsugi IJ, Kobayashi T. Examination of oxidation resistance of Mg_2Si thermoelectric modules at practical operating temperature. *J. Alloys Compd.* **735**, 828-832 (2018).
59. de Boor J, Gloanec C, Kolb H, Sottong R, Ziolkowski P, Müller E. Fabrication and characterization of nickel contacts for magnesium silicide based thermoelectric generators. *J. Alloys Compd.* **632**, 348-353 (2015).
60. Thimont Y, Lognoné Q, Goupil C, Gascoin F, Guilmeau E. Design of Apparatus for Ni/Mg_2Si and Ni/$MnSi_{1.75}$ Contact Resistance Determination for Thermoelectric Legs. *J. Electron. Mater.* **43**, 2023-2028 (2014).
61. Park SH, Kim Y, Yoo C-Y. Oxidation suppression characteristics of the YSZ coating on Mg_2Si thermoelectric legs. *Ceram. Int.* **42**, 10279-10288 (2016).
62. Zhu Q, Song S, Zhu H, Ren Z. Realizing high conversion efficiency of Mg_3Sb_2-based thermoelectric materials. *J. Power Sources* **414**, 393-400 (2019).
63. Zhao L-D*, et al.* Ultralow thermal conductivity and high thermoelectric figure of merit in SnSe crystals. *Nature* **508**, 373-377 (2014).
64. Zhao L-D*, et al.* Ultrahigh power factor and thermoelectric performance in hole-doped single-crystal SnSe. *Science* **351**, 141-144 (2016).
65. Chang C*, et al.* 3D charge and 2D phonon transports leading to high out-of-plane ZT in n-type SnSe crystals. *Science* **360**, 778-783 (2018).
66. Lee YK, Luo Z, Cho SP, Kanatzidis MG, Chung I. Surface oxide removal for polycrystalline SnSe reveals near-single-crystal thermoelectric performance. *Joule* **3**, 719-731 (2019).
67. Li J*, et al.* Substantial enhancement of mechanical properties for SnSe based composites with potassium titanate whiskers. *J. Mater. Sci.: Mater. Electron.* **30**, 8502-8507 (2019).
68. Burton MR*, et al.* 3D printed SnSe thermoelectric generators with high figure of merit. *Adv. Energy Mater.* **9**, 1900201 (2019).
69. Qin B*, et al.* Momentum and energy multiband alignment enable power generation and thermoelectric cooling. *Science*, eabi8668 (2021). doi: 10.1126/science.abi8668
70. Park SH, Jin Y, Ahn K, Chung I, Yoo C-Y. Ag/Ni metallization bilayer: a functional layer for highly efficient polycrystalline SnSe thermoelectric modules. *J. Electron. Mater.* **46**, 848-855 (2017).
71. Kim Y, Yoon G, Cho BJ, Park SH. Multi-layer metallization structure development for highly efficient polycrystalline SnSe thermoelectric devices. *Appl. Sci.* **7**, 1116 (2017).
72. Liu H*, et al.* Copper ion liquid-like thermoelectrics. *Nat. Mater.* **11**, 422 (2012).
73. He Y*, et al.* High Thermoelectric Performance in Non-Toxic Earth-Abundant Copper Sulfide. *Adv. Mater.* **26**, 3974-3978 (2014).
74. Stapfer G, Truscello VC. *Development of the data base for a degradation model of a selenide RTG*. Proceedings of the 12th intersociety energy conversion engineering conference. (American Nuclear Society, 1997)
75. Olvera AA*, et al.* Partial indium solubility induces chemical stability and colossal thermoelectric figure of merit in Cu_2Se. *Energy Environ. Sci.* **10**, 1668-1676 (2017).
76. Tang H*, et al.* Graphene network in copper sulfide leading to enhanced thermoelectric properties and thermal stability. *Nano Energy* **49**, 267-273 (2018).
77. Yang D*, et al.* Blocking Ion Migration Stabilizes the High Thermoelectric Performance in Cu_2Se Composites.

Adv. Mater. **32**, 2003730 (2020).

78. Brown SR, Kauzlarich SM, Gascoin F, Snyder GJ. $Yb_{14}MnSb_{11}$: New high efficiency thermoelectric material for power generation. *Chem. Mater.* **18**, 1873-1877 (2006).
79. Cerretti G, Villalpando O, Fleurial JP, Bux SK. Improving electronic properties and mechanical stability of $Yb_{14}MnSb_{11}$ via W compositing. *J. Appl. Phys.* **126**, 175102 (2019).
80. Vasilyeva IG, Nikolaev RE, Abdusaljamova MN, Kauzlarich SM. Thermochemistry study and improved thermal stability of $Yb_{14}MnSb$ alloyed by Ln^{3+} (La-Lu). *J. Mater. Chem. C* **4**, 3342-3348 (2016).
81. Black D*, et al.* Power Generation from Nanostructured Half-Heusler Thermoelectrics for Efficient and Robust Energy Harvesting. *ACS Appl. Energy Mater.* **1**, 5986-5992 (2018).
82. Macdonald RA, Macdonald WM. Thermodynamic properties of fcc metals at high temperatures. *Phys. Rev. B* **24**, 1715-1724 (1981).
83. Moruzzi VL, Janak JF, Schwarz K. Calculated thermal properties of metals. *Phys. Rev. B* **37**, 790-799 (1988).
84. Scudder MR*, et al.* Highly efficient transverse thermoelectric devices with Re_4Si_7 crystals. *Energy Environ. Sci.*(2021) doi.org/10.1039/D1EE00923K
85. Xie K, Gupta MC. High-Temperature Thermoelectric Energy Conversion Devices Using Si-Ge Thick Films Prepared by Laser Sintering of Nano/Micro Particles. *IEEE Trans. Electron Devices* **67**, 2113-2119 (2020).
86. Liu LC, Cao ZP, Chen M, Jiang J. Microstructure and Thermoelectric Properties of $(Bi_{0.48}Sb_{1.52})Te_3$ Thick Films Prepared with Tape Casting Method. *Electronics* **10**, 140 (2021).
87. Dong ZY*, et al.* Facile fabrication of paper-based flexible thermoelectric generator. *npj Flexible Electron.* **5**, 459 (2021).
88. Hikage Y*, et al.* Thermal expansion properties of thermoelectric generating device component. 2007 26th International Conference on Thermoelectrics. (IEEE, 2007)
89. Ferreres XR, Aminorroaya Yamini S, Nancarrow M, Zhang C. One-step bonding of Ni electrode to n-type PbTe — A step towards fabrication of thermoelectric generators. *Mater. Des.* **107**, 90-97 (2016).
90. Li G*, et al.* Micro- and Macromechanical Properties of Thermoelectric Lead Chalcogenides. *ACS Appl. Mater. Interfaces* **9**, 40488-40496 (2017).
91. Tan G*, et al.* All-Scale Hierarchically Structured p-Type PbSe Alloys with High Thermoelectric Performance Enabled by Improved Band Degeneracy. *J. Am. Chem. Soc.* **141**, 4480-4486 (2019).
92. Springholz G, Bauer G. 9.3.3 Substrate materials. In: *Growth and Structuring* (pp. 437-438). (Springer, Berlin, 2013)
93. Wu C-F, Wang H, Yan Q, Wei T-R, Li J-F. Doping of thermoelectric PbSe with chemically inert secondary phase nanoparticles. *J. Mater. Chem. C* **5**, 10881-10887 (2017).
94. Shi X*, et al.* Multiple-Filled Skutterudites: High Thermoelectric Figure of Merit through Separately Optimizing Electrical and Thermal Transports. *J. Am. Chem. Soc.* **133**, 7837-7846 (2011).
95. Rogl G*, et al.* New bulk p-type skutterudites $DD_{0.7}Fe_{2.7}Co_{1.3}Sb_{12-x}X_x$ (X=Ge, Sn) reaching ZT>1.3. *Acta Mater.* **91**, 227-238 (2015).
96. Ravi V*, et al.* Thermal Expansion Studies of Selected High-Temperature Thermoelectric Materials. *J. Electron. Mater.* **38**, 1433-1442 (2009).
97. Guo JQ*, et al.* Development of Skutterudite Thermoelectric Materials and Modules. *J. Electron. Mater.* **41**, 1036-1042 (2012).
98. Rogl G*, et al.* Thermal expansion of skutterudites. *J. Appl. Phys.* **107**, 043507 (2010).
99. Dahal T*, et al.* Thermoelectric and mechanical properties on misch metal filled p-type skutterudites $Mm_{0.9}Fe_{4-x}Co_xSb_{12}$. *J. Appl. Phys.* **117**, 055101 (2015).

100. Liu Z*, et al.* Mechanical properties of nanostructured thermoelectric materials α-MgAgSb. *Scr. Mater.* **127**, 72-75 (2017).
101. Hanninger G, Ipser H, Terzieff P, L. Komarek K. The Co-Sb phase diagram and some properties OF NiAs-type $Co_{1\pm x}Sb$. *Journal of the Less Common Metals* **166**, 103-114 (1990).
102. Fu C*, et al.* Realizing high figure of merit in heavy-band p -type half-Heusler thermoelectric materials. *Nat. Commun.* **6**, 8144 (2015).
103. Rogl G*, et al.* Mechanical properties of half-Heusler alloys. *Acta Mater.* **107**, 178-195 (2016).
104. Yu J*, et al.* Half-Heusler Thermoelectric Module with High Conversion Efficiency and High Power Density. *Adv. Energy Mater.* **10**, 2000888 (2020).
105. Mao J*, et al.* Manipulation of ionized impurity scattering for achieving high thermoelectric performance in n-type Mg_3Sb_2-based materials. *Proc. Natl. Acad. Sci.* **114**, 10548 (2017).
106. Liu Z*, et al.* Understanding and manipulating the intrinsic point defect in α-MgAgSb for higher thermoelectric performance. *J. Mater. Chem. A* **4**, 16834-16840 (2016).
107. Agne MT*, et al.* Heat capacity of Mg_3Sb_2, Mg_3Bi_2, and their alloys at high temperature. *Mater. Today Phys.* **6**, 83-88 (2018).
108. Li J*, et al.* Point defect engineering and machinability in n-type Mg_3Sb_2-based materials. *Mater. Today Phys.*, 100269 (2020).
109. Martinez-Ripoll M, Haase A, Brauer G. The crystal structure of α-Mg_3Sb_2. *Acta Crystallogr., Sect. B* **30**, 2006-2009 (1974).
110. Wiedemeier H, Csillag FJ. The thermal expansion and high temperature transformation of SnS and SnSe. *Zeitschrift für Kristallographie - Crystalline Materials* **149**, 17 (1979).
111. Liu G, Zhou J, Wang H. Anisotropic thermal expansion of SnSe from first-principles calculations based on Grüneisen's theory. *Phys. Chem. Chem. Phys.* **19**, 15187-15193 (2017).
112. Tyagi K*, et al.* Crystal structure and mechanical properties of spark plasma sintered Cu_2Se: An efficient photovoltaic and thermoelectric material. *Solid State Commun.* **207**, 21-25 (2015).
113. Ding YF*, et al.* High performance n-type Ag_2Se film on nylon membrane for flexible thermoelectric power generator. *Nat. Commun.* **10**, 1-7 (2019).
114. Rauscher JF*, et al.* Synthesis, structure, magnetism, and high temperature thermoelectric properties of Ge doped $Yb_{14}MnSb_{11}$. *Dalton Trans.* **39**, 1055-1062 (2010).
115. Liu Y, Xie H, Fu C, Snyder GJ, Zhao X, Zhu T. Demonstration of a phonon-glass electron-crystal strategy in (Hf,Zr)NiSn half-Heusler thermoelectric materials by alloying. *J. Mater. Chem. A* **3**, 22716-22722 (2015).
116. Zhao L-D, Zhang B-P, Li J-F, Zhou M, Liu W-S, Liu J. Thermoelectric and mechanical properties of nano-SiC-dispersed Bi_2Te_3 fabricated by mechanical alloying and spark plasma sintering. *J. Alloys Compd.* **455**, 259-264 (2008).
117. Zheng Y*, et al.* Mechanically Robust BiSbTe Alloys with Superior Thermoelectric Performance: A Case Study of Stable Hierarchical Nanostructured Thermoelectric Materials. *Adv. Energy Mater.* **5**, 1401391 (2015).
118. Kim SI*, et al.* Dense dislocation arrays embedded in grain boundaries for high-performance bulk thermoelectrics. *Science* **348**, 109 (2015).
119. Zhu B*, et al.* Realizing record high performance in n-type Bi_2Te_3-based thermoelectric materials. *Energy Environ. Sci.* **13**, 2106-2114 (2020).
120. Fu L*, et al.* Large enhancement of thermoelectric properties in n-type PbTe via dual-site point defects. *Energy Environ. Sci.* **10**, 2030-2040 (2017).
121. Tan G*, et al.* Non-equilibrium processing leads to record high thermoelectric figure of merit in PbTe–SrTe.

Nat. Commun. **7**, 1-9 (2016).
122. Zhao H*, et al.* High thermoelectric performance of MgAgSb-based materials. *Nano Energy* **7**, 97-103 (2014).
123. Wang BL, Guo YB, Zhang CW. Cracking and thermal shock resistance of a Bi_2Te_3 based thermoelectric material. *Eng. Fract. Mech.* **152**, 1-9 (2016).
124. Pavlova LM, Shtern YI, Mironov RE. Thermal expansion of bismuth telluride. *High Temp.* **49**, 369-379 (2011).
125. Kirkham MJ, dos Santos AM, Rawn CJ, Lara-Curzio E, Sharp JW, Thompson AJ. Abinitio determination of crystal structures of the thermoelectric material MgAgSb. *Phys. Rev. B* **85**, 144120 (2012).
126. Wang J-F, Fu X-N, Zhang X-D, Wang J-T, Li X-D, Jiang Z-Y. Structural, elastic, electronic, and thermodynamic properties of MgAgSb investigated by density functional theory. *Chin. Phys. B* **25**, 086302 (2016).

Acknowledgements

TE materials research at NTU is supported by Singapore MOE AcRF Tier 2 under Grant Nos. 2018-T2-1-010, Singapore A*STAR Pharos Program SERC 1527200022, Singapore A*STAR project A19D9a0096. TE materials research at Northwestern University is supported by the U.S Department of Energy, Office of Science and Office of Basic Energy Sciences for funding under award number DE-SC0014520.

Author contributions

The manuscript was written through contributions from all authors. All authors have approved the final version of the manuscript.

Competing interests

The authors declare no competing interests.

Additional information

Reprints and permissions information is available at www.nature.com/reprints.

Correspondence should be addressed to MGK (m-kanatzidis@northwestern.edu)

Publisher's note: Springer Nature remains neutral with regard to jurisdictional claims in published maps and institutional affiliations.

Table I. Summary of properties and device conversion efficiency of discussed materials

Material	Peak ZT	Linear Thermal Expansion ($\times10^{-6}$ K^{-1})	Vickers Hardness	Fracture Toughness	PCE (%)	Melting/Decomposition Point	Operation Temperature range
PbTe-based	1.4 (n)[24] 2.2 (p)[24]	$\alpha_{373-773\ K}$ = 19 to 20 (n & p) *i) [88, 89]	0.3 GPa [33, 90]	0.59 MPa $m^{1/2}$ [33, 90]	14.0 (n)[24] (T_{cold} = 323 K, T_{hot} = 773 K)	1190-1210K	500-900K
PbSe-based	1.8 (n)[30] 1.7(p)[91]	α_{300K} = 19.4 (n & p) *i) [92]	0.18 GPa[93]	0.67 MPa $m^{1/2}$ [90]	12.3 (n)[30] (T_{cold} = 293 K, T_{hot} = 800 K)	1340-1350K	600-1000K
Skutterudite-based	1.7 (n)[94] 1.45 (p)[95]	$\alpha_{473-873\ K}$ = 10 to 12.2 *ii),[96, 97, 98] 14.5 *iii)[96]	4.2 GPa [99]	1.49 MPa $m^{1/2}$ [100]	9.1 (n)[40] (T_{cold} = 323 K, T_{hot} = 923 K)	1137-1147K[101]	500-900K
Half-Heusler-based	1.0 (n)[102] 1.5 (p)[102]	$\alpha_{200-800\ K}$ = 8.6 to 12.1 *iv),[103, 104] 10.6 to 12.9 *v)[103, 104]	8.5-14.4 GPa [103]	2.1 MPa $m^{1/2}$ [103]	6.2 (p)[102] (T_{cold} = 336 K, T_{hot} = 991 K)	--	>900K
Mg_3Sb_2-based	1.7 (n)[105] 1.3 (p)[106]	$\alpha_{300-773\ K}$ = 22.3 (n & p) *i)[107]	1.1 GPa [108]	1.4 MPa $m^{1/2}$ [108]	10.6 (n)[62] (T_{cold} = 373 K, T_{hot} = 773 K)	1508-1528K[109]	500-900K
SnSe-based	2.8 (n)[65] 2.6 (p)[63]	$\alpha_{200-800\ K}$ = 13 to 14.9 (n & p) *i)[110, 111]	0.67 GPa [67]	0.62 MPa $m^{1/2}$ [67]	--	1120-1140K	>900K

Cu_2Se-based	2.7 (p)[77]	$\alpha_{773-1000\ K}$ = 107 [72]	0.43 GPa [112]	2 MPa $m^{1/2}$ [112]	9.1 (p)[113] (T_{cold} = 300 K, T_{hot} = 973 K)	1376-1396K	>900K
$Yb_{14}MnSb_{11}$	1.3 (p)[79]	--	>3 GPa [79]	--	--	>1200K[114]	>900K

*Notes: **i)* Chemical composition and thermal expansion coefficient data are very similar for both n- and p-type variations. **ii)* For n-type filled $CoSb_3$-based skutterudites. **iii)* For p-type filled $FeSb_3$-based skutterudites. **iv)* For n-type (Ti,Zr,Hf)NiSn-based Half-Heusler alloys. **v)* For p-type Ti(Fe,Co)Sb-based Half-Heusler alloys.

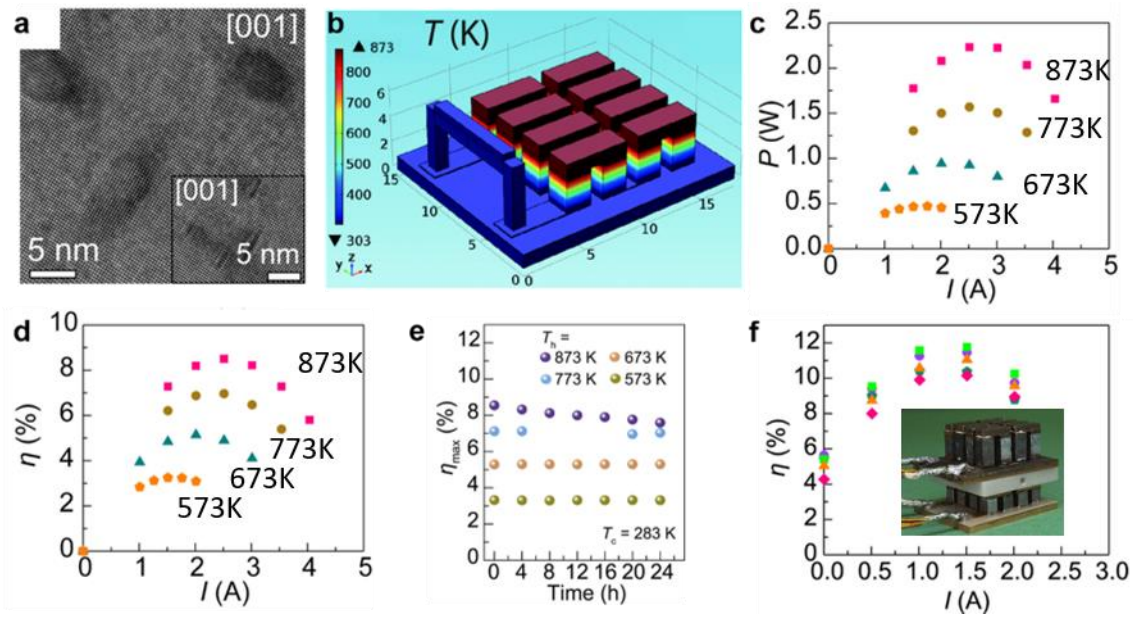

Fig. 1 | The power and conversion efficiency of PbTe based modules. **a,** High-resolution TEM image of $Pb_{0.953}Na_{0.040}Ge_{0.007}Te$ showing nanoprecipitates and disk-like nanostructures (inset) in the [001] zone axis; **b,** Typical results of numerical simulations for the nanostructured PbTe-based module (PbTe–2% MgTe doped with 4% Na (p-type) and PbTe doped with 0.2% PbI_2 (n-type)) for hot side at 873 K and cold side at 303 K and load conductivity of 4.5×10^2 S cm^{-1}. Dimensions of the module are in mm; **c,** Electrical power output (P) and **d,** Conversion efficiency (η) of the nanostructured PbTe-based module as function of electrical current (I). The hot-side temperature (T_h) was changed from 873 K to 573 K, while the cold-side temperature (T_c) was maintained at 283 K; **e,** η_{max} as a function of time (hours) for 24-hr testing with T_h = 873, 773, 673, and 573 K and T_c = 283 K of Nanostructured PbTe-Based Module; **f,** PCE (η) as function of current (I) of the nanostructured $Pb_{0.953}Na_{0.040}Ge_{0.007}Te$ module cascaded with a Bi_2Te_3 module (inset). T_h and T_c were at 873 K and 283 K, respectively. The measurements were performed at various currents (2.0−4.0 Amp). [22, 23] Copyright 2015, The Royal Society of Chemistry & Copyright 2020, Cell Press.

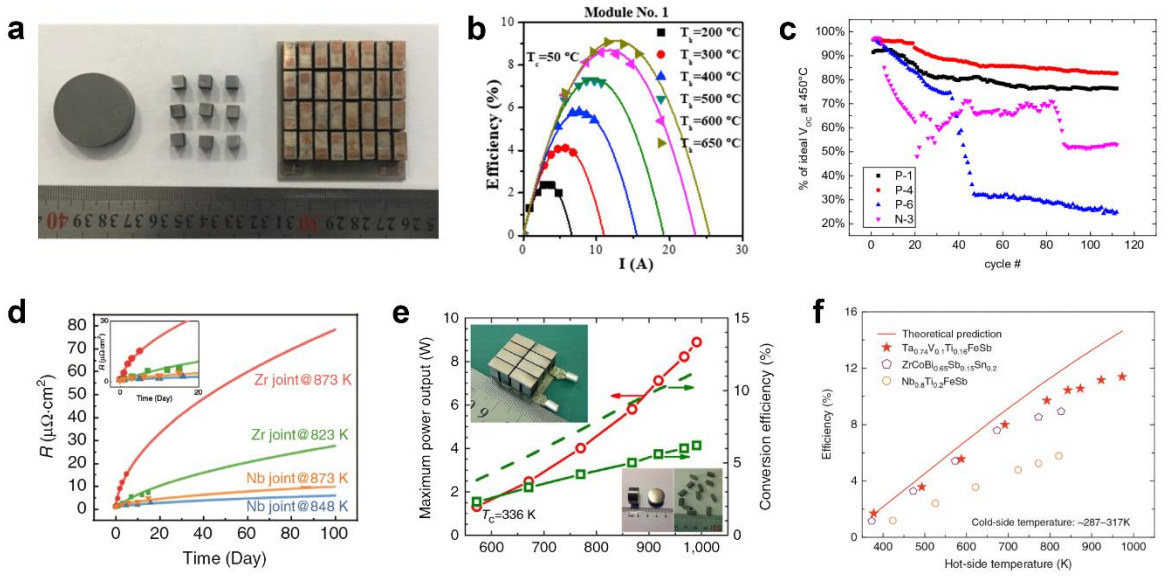

Fig2. | The conversion efficiency and stability of skutterudite based modules. **a,** An 8×8 leg device made from n-type $CoSb_3$ (filled with Yb, Ca, Al, Ga, *ZT* ~1.2) and p-type $CoSb_3$ (filled with Pr, Ti, Ga, Ba, Fe, *ZT* ~0.85). **b,** energy conversion efficiency with different hot side temperatures, T_{hot}. The cold side temperature is kept at 50 °C (323K).[40] **c,** Change of open circuit voltages V_{oc} of four skutterudite legs upon thermal cycling. The hot sides are cycled between 150 °C (423 K) and 500 °C (773 K) and the cold sides are cycled between 25 °C (298 K) and 50 °C (323 K). [42] **d,** Interfacial resistivity *R* for skutterudite/Nb and skutterudite/Zr joints after aging at 823 K and 873 K for different days. Dots are experimental data and lines are numerical curve fitting.[43] **e,** Maximum power output (P_{max}) and PCE (η) as a function of hot side temperature (T_H) for a TE device made from $FeNb_{0.88}Hf_{0.12}Sb$ and ZrNiSn. The dash line represents the theoretical conversion efficiency assuming no electrical and thermal contact resistances.[47] **f,** Measured hot-side temperature-dependent heat-to-electricity PCE of $Ta_{0.74}V_{0.1}Ti_{0.16}FeSb$ and $ZrCoBi_{0.65}Sb_{0.15}Sn_{0.2}$.[49] (add copy right)

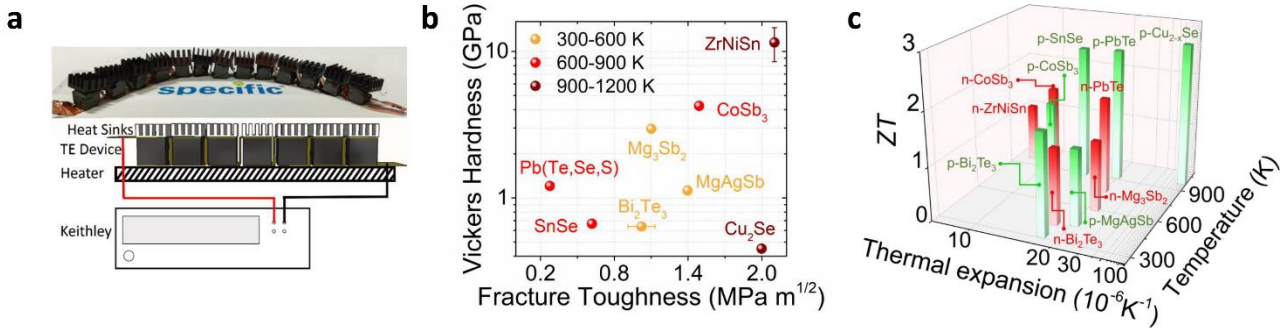

Fig3. | A SnSe based modules and summaries of mechanical and thermal properties of TE materials. **a,** 3D printed SnSe thermoelectric power generator.[68] **b,** Histogram of peak ZT, Vickers Hardness and Fracture Toughness of bulk polycrystalline ZrNiSn,[47, 103, 115] $CoSb_3$,[94, 95, 99, 100] Bi_2Te_3,[116, 117, 118, 119] SnSe,[66, 67] Cu_2Se,[77, 112] PbTe,[33, 90, 120, 121] Mg_3Sb_2,[106, 108] and MgAgSb.[100, 122] As shown in the legend, the data bars of each material are colour-coded according to the temperature range of their peak ZTs. The Vickers Hardness values are plotted using a log scale. The error bar of the Vickers of the ZrNiSn-based Half-Heusler alloys were determined for samples with different doping compositions. **c,** Plot of

thermal expansion coefficient data and peak ZT of bulk polycrystalline $CoSb_3$,[94, 95, 96, 97, 98] ZrNiSn,[103, 115] Bi_2Te_3,[118, 119, 123, 124] SnSe,[66, 110, 111] Cu_2Se,[72, 77] PbTe,[88, 89, 120, 121] Mg_3Sb_2,[106, 107] and MgAgSb.[122, 125, 126] As shown in the legend, the data points of each material are colour-coded according to the temperature range of their peak ZTs. The thermal expansion coefficient is plotted using a log scale. (Add copy right)

Box 1

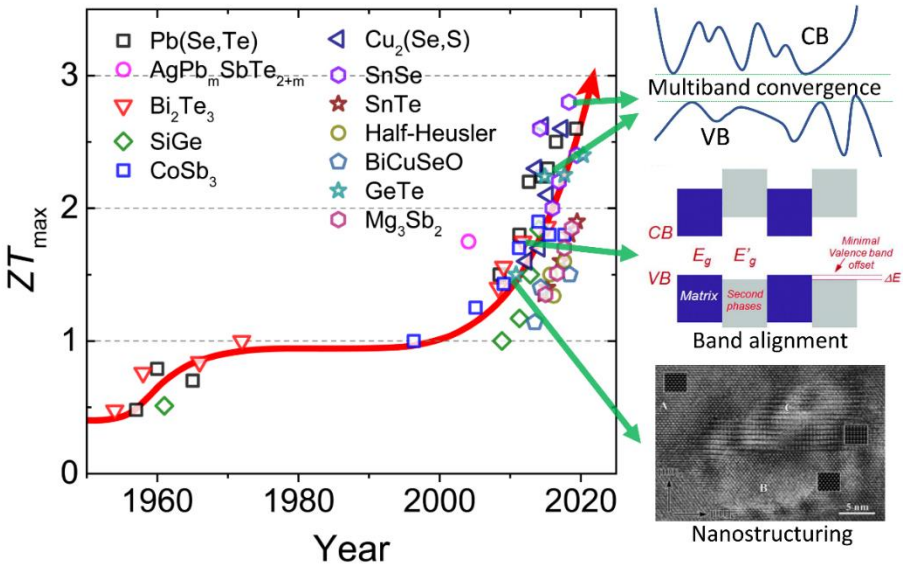

Figure | Decadal timeline and progress in raising the efficiency of thermoelectric materials through successive innovations since around 2000. The red line is drawn as a guide to the eye. On the right side some of the key Innovations in materials design concepts that let these advances are shown schematically.

In-situ inclusion of nanostructures are of great importance in improving TE performance. Nano precipitates of a second phase are caused to grow in the TE material which acts as the host matrix. These dispersed nano-sized objects act as efficient phonon scattering centers, strongly impeding heat flow. During the nucleation and growth, the interface created between the host matrix and the precipitates should be as coherent as possible which is referred to as endotaxy. Electronic band alignment between the two phases is necessary to easily transmit charge carriers especially in an endotaxial interface. This arrangement can effectively scatter phonons and at the same time allow charge carrier to pass through with ease. This strategy requires the creation of special heterogeneous materials. when the heterogeneity scale extends beyond the nano-sized regime (e.g. 5-50 nm) and into what we call the meso scale (50-1000 nm) then additional heat-carrying phonon can be scattered whose mean free paths are comparable to those of the scale. In that case we have an all-scale architecture that can scatter a broad spectrum of phonons. The all-scale architecture is the most effective composite structure for many thermoelectric systems.

Multiband convergence is when the electronic conduction (CB) or valence band (VB) extrema in a given electronic structure of a thermoelectric material occur multiple times and fall within a small energy range. For example when an electronic structure has only one extremum it generally is considered to be inferior from the thermoelectric performance point of view than a corresponding structure that has multiple. The presence of many such band extrema can enable the achievement of very high power factors. When electron or hole pockets are created through doping in each individual band extremum of the CB or VB, each pocket contributes to the power factor in roughly an additive manner (see ref 11 for a more extensive discussion).